Received: 12 April 2021 | Revised: 2 November 2021 | Accepted: 12 November 2021

DOI: 10.1002/eqe.3582

RESEARCH ARTICLE

WILEY

Artificial neural network application in predicting probabilistic seismic demands of bridge components

Farahnaz Soleimani[1] | **Xi Liu**[2]

[1] Department of Civil and Environmental Engineering, Georgia Institute of Technology, Atlanta, GA, USA

[2] Machine learning Department, Intuitive Surgical, Atlanta, GA, USA

Correspondence
Farahnaz Soleimani, Department of Civil and Environmental Engineering, Georgia Institute of Technology, Atlanta, GA, USA.
Email: soleimani@gatech.edu

Abstract

Probabilistic seismic demand models (PSDMs) of bridge components such as column and abutment are commonly developed through classical linear regression techniques in which a univariate model format is predefined in the logarithmically transformed space. The more advanced machine learning (ML)-based PSDMs incorporate various sources of uncertainties, which eventually leads to a more credible prediction of the seismic demands of bridge components and enhances the vulnerability assessment of the overall bridge systems. Despite the emerging advancements in ML approaches, many of them have not yet been introduced to estimate bridge seismic responses. To this end, the present study seeks to develop predictive PSDMs using a reputable ML approach, the artificial neural network (ANN). Relative to the classical univariate PSDMs, the ANN-based PSDMs improve the median estimation of demands, particularly over the large and small range of ground motion intensities and reduce the total prediction variability. Moreover, the proposed ANN-based approach provides a generalizable model with an unbiased prediction of the seismic demands. The ANN-based PSDMs can be further used in estimating the probability of structural damage in the fragility and risk assessment process.

KEYWORDS

artificial neural network, concrete box-girder bridge, machine learning, performance-based analysis, probabilistic seismic demand model

1 | INTRODUCTION

Proper prediction of the component demands of bridges subjected to earthquake excitations is essential for reliable performance-based assessment of highway bridges and eventual hazard decision-makings. This seismic hazard prediction is typically assessed by deriving analytical probabilistic seismic demand models (PSDMs) for bridge components including column, deck, foundation, and abutment. The PSDMs are commonly utilized to generate analytical fragility curves of a bridge system, and these curves are further used in the earthquake resilience assessment of a transportation network. The most well-known and widely used PSDM is a single parameter regression model[1] that estimates demand as a function of ground motion intensity measure (IM) (e.g., peak ground acceleration (PGA)). Most of the previously developed bridge PSDMs have used the classical format, although more recently generated models investigated alternative formats. Although the classical model is simple to implement, it can be improved in several aspects to enhance the reliability and prediction power of the model. As indicated by previous studies (Seo & Linzell, 2013; Ghosh et al., 2013; Soleimani et al.,[2–4];

Xie et al., 2019[5]) based on data-driven approaches, this classic model can be improved by including more input variables (e.g., span length, column height, concrete strength) that represent additional sources of uncertainties[6] in the regression model and investigating alternative regression equations (e.g., 2nd order polynomial). A few researchers (e.g., Soleimani et al., 2017[4]; Xie & DesRoches, 2019[7]) incorporated feature selection techniques (e.g., LASSO and stepwise regression) to identify the most influential uncertain parameters in estimating the bridge component demands. These studies yet expressed the demands as a linear function of the random variables after transferring them to a logarithmic scale. The findings from these studies and several other sensitivity studies revealed the importance of the inclusion of structural geometries uncertainty along with the ground motion parameters in estimating the probabilistic seismic demands[8] and fragility curves[9] of highway bridges. Neglecting these significant sources of uncertainties could lead to over- or underestimation of the seismic demands of bridge components.

Some other researchers considered response surface models, mostly the 2nd-order polynomial regression model, as an alternative functional form for the PSDMs. In this regard, Pan et al.[10] found the 2nd-order regression model more efficient than the multivariate linear regression model for fitting the response data of a multi-span I-girder steel highway bridge, particularly for ground motions stronger than 0.6 g (PGA). Their study was limited to specific input regression parameters. More specifically, they used ground motion moment magnitude and distance as the input variables of the multivariate model, while they used a single parameter PGA in their quadratic model. Furthermore, Seo and Park[11] developed fragility curves for a portfolio of regional curved steel I-girder bridges in the Eastern United States. They used PGA as the ground motion intensity and expressed the bridge component demands such as the curvature ductility of the bridge columns using a 2nd-order polynomial model.

Although a growing body of research has been evolved over the recent years to propose alternative approaches to develop PSDMs, none has been proved to be dominantly superior over other approaches. There yet remains challenges to be addressed by future research to enrich predictions provided by PSDMs and expanding their application beyond certain methodology. Furthermore, each study is limited to a specific bridge type, a selective number of random variables as the predictors, fixed functional forms, and assumptions.

The classical regression techniques used to develop PSDMs suffer from several drawbacks such as the fixed functional forms, low prediction power to capture nonlinearity, and prior assumption on the lognormality distribution of the demands. More specifically, this method necessitates a predefined functional form for the regression model. These presumed equational forms may incorporate a simple format such as a linear model with single parameter, multivariable linear model, or a more complex format such as the polynomial regression. For example, in the classical unidimensional form, the seismic demand is conditioned on a single parameter as the seismic IM. However, a more general trend and complex interaction between the input and output variables may not be accurately captured by the classical regression technique due to the high-dimensional nonlinear nature of the PSDMs. In addition, the lack of flexibility to incorporate various sources of uncertainties into the formulation of PSDM influences the reliability of the estimation of the demands. For example, the uncertainties associated with structural modeling parameters are not incorporated in the formulation of the unidimensional PSDM. Hence, evaluating the impact of the variations of these parameters on the demands requires substantial computational cost for reanalyzing the bridge with the new set of parameter combinations. Therefore, including a variety of uncertain configurational features in the list of input variables of the PSDM is crucial for a more realistic estimation of the demands. Besides, an assumption of a particular distribution for the demands (e.g., the lognormality assumption in the single parameter regression model) poses subjective bias on the predictions. The distribution of demands is often unknown, while the predefined distribution may not be compatible for all engineering demand parameters (EDPs) and different classes of bridges as shown by a couple of recent studies.[12,13] As a result, a more generalized approach in which the algorithm is not restricted to a fixed functional form and a particular assumption on the distribution of the parameters would be more desirable for practical application. To tackle these challenges, a powerful alternative to the classic regression techniques is implementing modern machine learning (ML) approaches.

Given the growing advances in computational technologies, ML approaches provide a tremendous potential (e.g., handling large-scale data, dealing with complex problems and data scarcity, proposing computationally efficient solutions) to enhance predictive seismic analysis.[14] However, despite the existing variety of ML algorithms and their applications in different disciplines, the implementation of ML in improving the probabilistic seismic analysis of bridges is in its early stages. In particular, further research is required to leverage the benefits that modern ML methods could offer for the prediction of bridge demands. Among these methods, artificial neural network (ANN) has received increasing interest over the years thanks to its robustness and flexibility[14,15]; however, its application in the context of PSDMs is rather very limited. ANN can outperform other ML methods owing to its capability to capture the high-dimensional nonlinear relationship between the predictors and the EDPs. Because of the hidden layers and various activation functions,

ANN can be especially helpful to model the nonlinearities within the dataset compared to a regression model. In addition, ANN can also model more complicated relationships between the input and output data without engineered prior knowledge.

During the past decades, ANN has been applied to fragility assessment for steel moment-resisting frames,[16] 3D reinforced concrete buildings,[17] masonry building,[18] electrical cabinets of nuclear power plants,[19] masonry veneers,[20] and nonlinear hysteretic systems.[21] Within the seismic assessment of bridges, Pang et al.[22] showed that implementing ANN helps to reduce intensive computations that are involved in generating fragility curves of highway bridges. They tested the efficiency of the ANN approach on a three-span continuous bridge, which is a common bridge type in China and chose PGA as the ground motion IM. Likewise, Mangalathu et al.[9] proposed ANN to eliminate unnecessary grouping of bridge classes based on their fragilities. By studying skewed concrete bridges with seat abutments, they found that prior grouping of bridges is not required using the ANN-based model, and better fits with a higher coefficient of determination and lower mean square error can be obtained compared to the classical fragility analysis approach. These studies used one hidden layer and a certain pre-assumed number of nodes in the layer. Researchers reported that the ANN model specifications such as the number of hidden layers and the number of nodes will influence the efficiency of the ANN algorithm.[23] Although it is expected that the estimated seismic demand values of bridge components significantly depend on these characteristics, implemented algorithms, and associated uncertain parameters, their impact is still unclear on the overall probabilistic seismic analysis, since previous studies that applied ANN only used one hidden layer and assumed a particular number of nodes for their analysis without performing a sensitivity analysis.

The review of the literature indicates that the classical regression-based PSDMs need to be improved to better estimate the seismic vulnerability of bridges. Since the ANN has rarely been applied for the seismic performance assessment of highway bridges, this study aims to improve the knowledge regarding the application of the ANN algorithm to estimate the seismic demands of bridge components. In summary, this study aims to address three main challenges in building PSDMs in a single framework: (I) whether stochastic gradient descent ANN is a suitable approach for developing PSDMs? (II) What type of ANN architecture (in terms of the number of neurons and solvers methodologies) is more suitable for predicting the seismic demands of bridge components? Do additional hidden layers significantly impact the results? (III) How much are the predictions improved using the ANN-based model compared to the classic PSDMs? (IV) Does this approach provide comparable results to the multiparameter linear and 2nd-order regression models?

Although previous efforts provide valuable insight into the general effectiveness of ANN application in the seismic assessment of bridges, there is a lack of systematic appraisal of different tools that can be used to optimize the efficacy of the ANN model to ensure the efficient and generalizable performance of the ANN in developing bridge PSDMs. To address these shortcomings, this study designs an ANN framework for bridge-specific PSDMs and seeks to identify the effect of the ANN model characteristics such as network hyperparameters and optimization solvers on PSDM accuracy to determine the most suitable specifications. The model utilized in the ANN predictions is compared with the results from the common regression-based PSDMs including the unidimensional, multiparameter, and polynomial regression models. The proposed ANN approach is shown to be capable of producing simplified mathematical expressions while taking into consideration a comprehensive list of inherent uncertainties and data complexity.

2 | BRIDGE SEISMIC DEMAND DATABASE

This study investigates the seismic demands of key bridge components including column, deck, foundation, and abutment.[24] To this end, representative bridge models for the class of multi-span box-girder concrete bridges (Figure 1) are created in Opensees[25] and dynamic time-history analyses are conducted on the bridge finite element models. These bridges are under the category of tall pier bridges with three different ranges of column height ratios including low, medium, and high.[26] For a detailed description of the bridge model, interested authors are encouraged to check the work by Soleimani[27] since the same modeling strategies and characteristics for the considered bridges are followed in this study. Bridge samples are created using the distribution of parameters (Table A.1 – Appendix A) using the Latin Hypercube sampling technique. A wide-ranging set of 160 ground motions with two scaling factors of 1 and 2 (resulting in a total of 320 excitations) is selected from Baker's ground motion database.[28] Performing seismic analysis by applying 320 ground motions on the three classes of tall bridges leads to a total nonlinear time history analysis of 960 combinations of bridge samples and ground motions. For each excitation, the maximum demands of the bridge components are recorded at the end of shaking, resulting in a total of 5760 seismic demand databases.

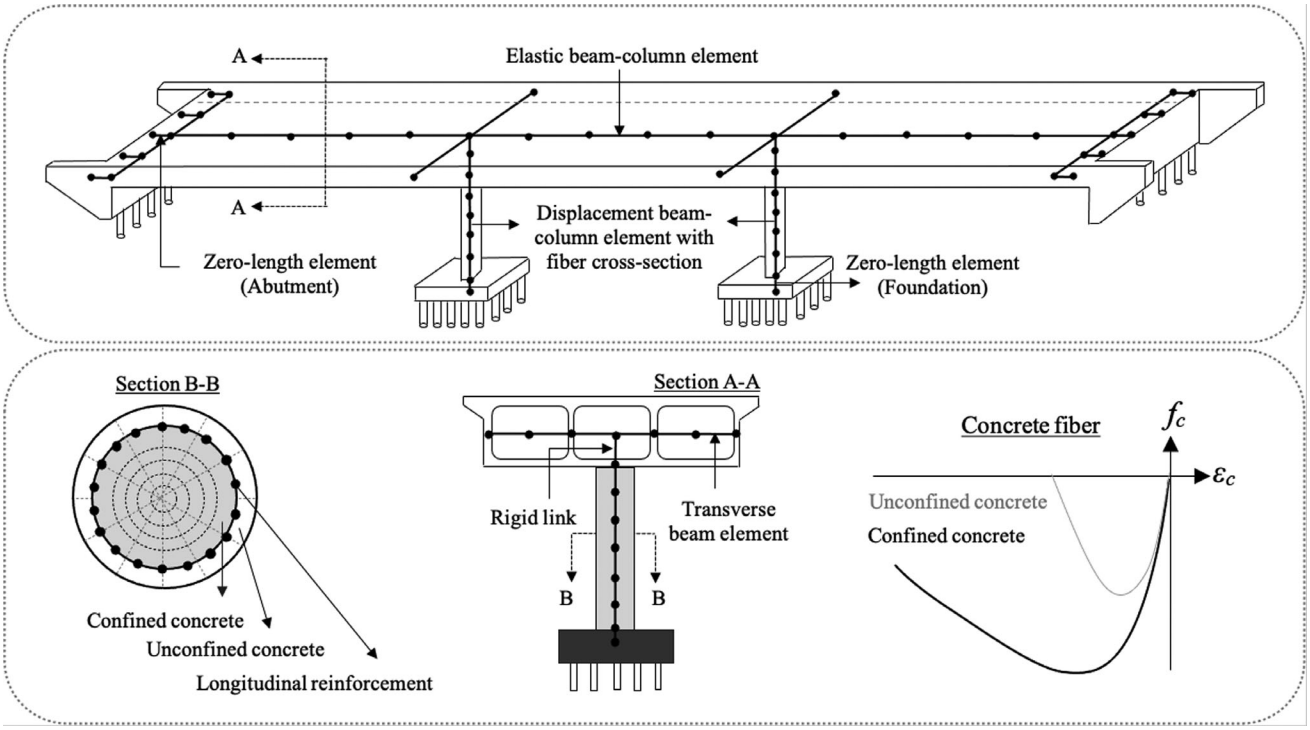

FIGURE 1 Schematic layout of the bridge models

3 | DEVELOPMENT OF ANN MODEL

3.1 | ANN framework

This study applies ANN algorithms[29–31] and utilizes modern deep learning tools to train the models. This study implements the gradient descent algorithm and conducts backpropagation.[32–35] As displayed in a schematic diagram in Figure 2, the neural network consists of at least three layers: an input layer, an output layer, and single or multiple hidden layers. The input layer is built upon the input variables that are used in the prediction models. For this study, the input variables include ground motion properties, structural and modeling parameters listed in Table 1. The first eight variables that are the categorical types are binary coded, and the remaining numerical variables are used in the models after transferring them to the natural logarithmic space. The output layer represents the seismic demand predictions, as provided in Table 2, in the natural logarithmic scale.

The interaction between the layers is demonstrated in Figures 3 and 4. The hidden layer is comprised of neurons that link the input to the output dataset. In the process of transferring from the input layer to the ith neuron in the hidden layer, the input variables are multiplied by weights and added by a bias factor. Then, a nonlinear activation function is applied to the results to generate the output values of the ith neuron in the hidden layer. To link the data from the hidden layer to the output layer, another set of weights, bias, and activation functions are applied to the hidden layer data. Using a back-propagation algorithm,[36] weights and biases are optimized.

In the gradient descent algorithm, the vector of weights and biases (i.e., $\boldsymbol{\lambda}_t$) is updated through an optimization process. At each iteration, this algorithm takes steps in the negative direction of the gradient of the loss (i.e., $\nabla_{\boldsymbol{W},\boldsymbol{B}} L(\boldsymbol{\lambda}_{t-1})$ where L represents the loss function with respect to the weight ($\boldsymbol{W}$) and bias ($\boldsymbol{B}$). The network parameters at the iteration number t with the learning rate of α are computed as in Equation (1). At each optimization iteration, a unique subset of training data is used.

$$\boldsymbol{\lambda}_t = \boldsymbol{\lambda}_{t-1} - \alpha \nabla_{\boldsymbol{W},\boldsymbol{B}} L\left(\boldsymbol{\lambda}_{t-1}\right) \tag{1}$$

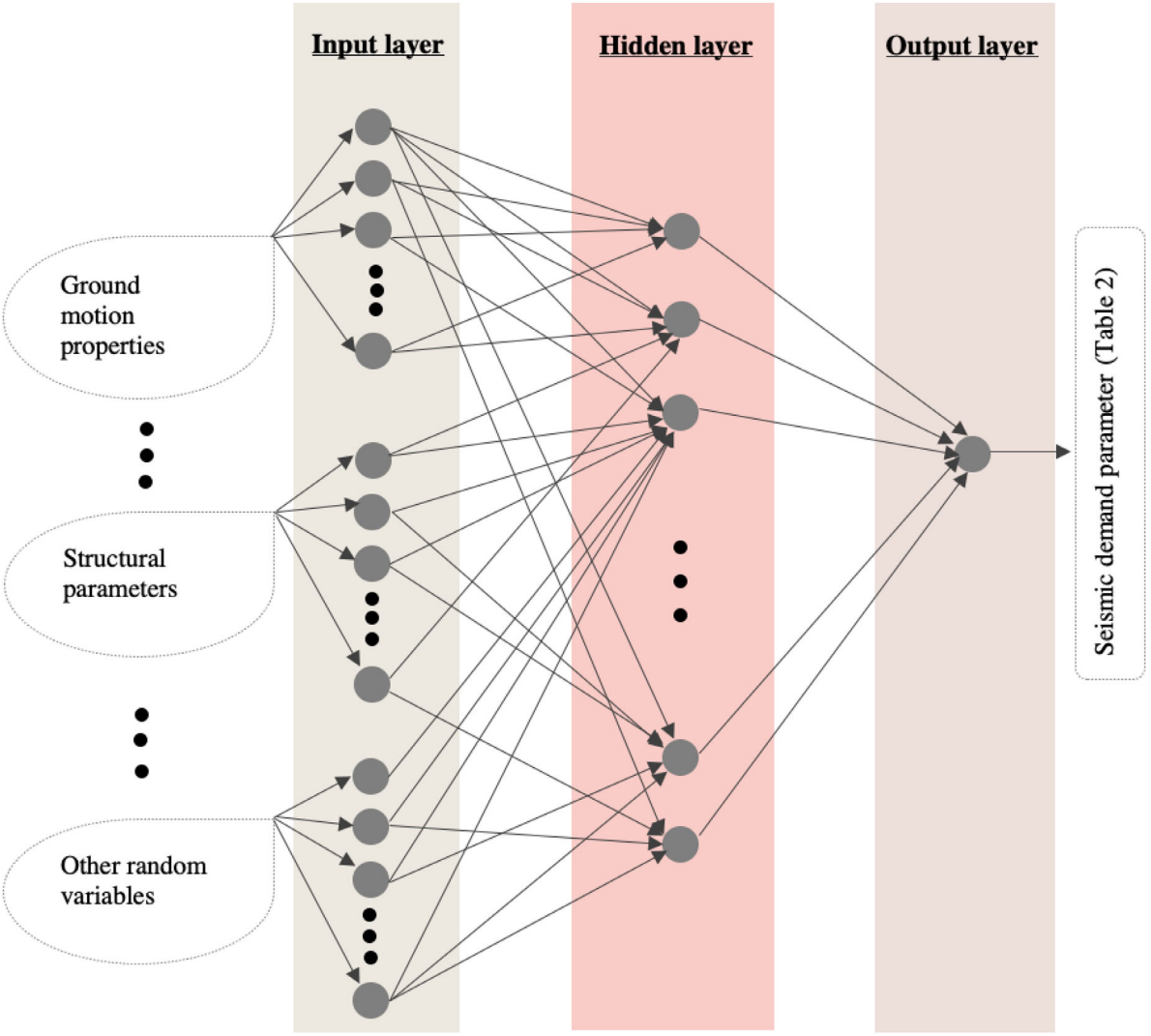

FIGURE 2 General artificial neural network (ANN) framework

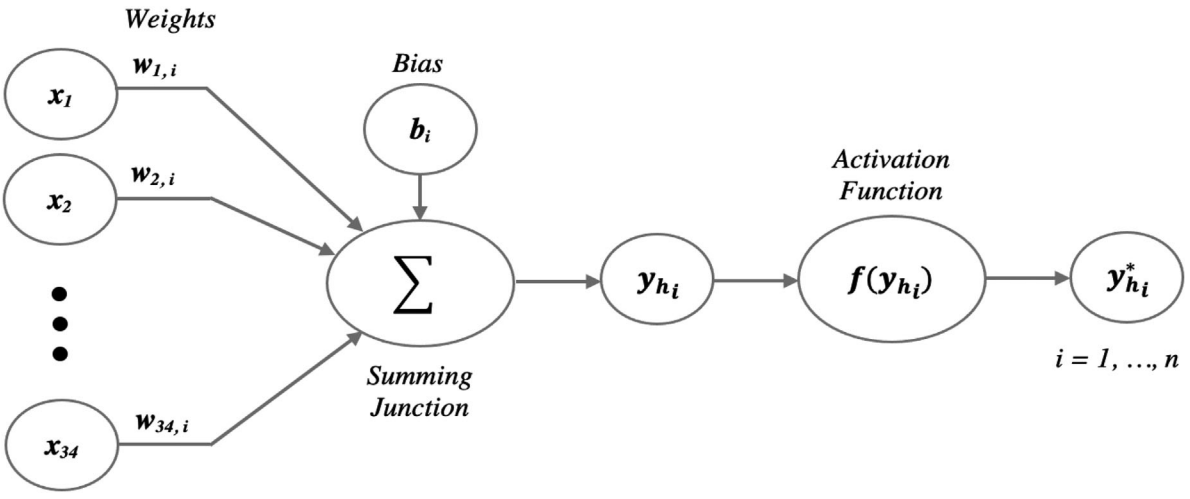

FIGURE 3 Transaction from input layer variables to the *i*th neuron in the hidden layer

TABLE 1 List of input variables considered for the artificial neural network (ANN) approach

Input variables	Seismic analysis characteristic	Input variables	Seismic analysis characteristic
x_1	Soil type	x_{18}	Foundation rotational stiffness (translational direction)
x_2	Girder type	x_{19}	Foundation rotational stiffness (longitudinal direction)
x_3	Column cross-section shape	x_{20}	Foundation translational stiffness
x_4	Abutment type	x_{21}	Concrete strength
x_5	Footing type	x_{22}	Reinforcement strength
x_6	Fixity type	x_{23}	Mass
x_7	Direction of excitations	x_{24}	Damping
x_8	Number of spans	x_{25}	Span ratio
x_9	Span length	x_{26}	Column height ratio
x_{10}	Column height	x_{27}	Ground motion dt
x_{11}	Deck width	x_{28}	PGA
x_{12}	Number of cells in the box-girder	x_{29}	Sa (1.0 s)
x_{13}	Girder space	x_{30}	Sa (0.2 s)
x_{14}	Top flange thickness	x_{31}	Sa (0.3 s)
x_{15}	Superstructure Depth	x_{32}	Mw
x_{16}	Reinforcement ratio	x_{33}	R
x_{17}	Abutment height	x_{34}	Vs30

TABLE 2 Seismic demand parameters to predict

Predicted variable	Seismic demand
y_1	Column curvature ductility
y_2	Deck displacement
y_3	Foundation translational displacement
y_4	Foundation rotation
y_5	Active abutment displacement
y_6	Passive abutment displacement

3.2 | Tuning of hyperparameters

The network architecture is defined according to the number of hidden layers along with the number of neurons in these layers. The network architecture and the implemented solver (e.g., Adam optimizer) to optimize the gradient descent network could significantly control the predictive power of the ANN-based PSDM,[23,37] Therefore, a sensitivity study is conducted to identify the influence of the network architecture and the type of algorithm on the model performance. Based on evaluating the prediction accuracy and the mean squared errors (MSEs), the most-viable set of hyperparameters for the final model is determined.

A set of options was tested for training the neural network using gradient descent. Three common solvers including Adam optimizer,[38] stochastic gradient descent with momentum (SGDM),[39] and root mean squared propagation (RMSProp) optimizer[40] are evaluated for training networks. The SGDM adds an additional momentum term ($\tau(.)$) to Equation (1) to incorporate the contribution of the gradients from the last steps and dampen oscillation around local optima to accelerate gradients in the relevant direction towards the optimum (see Equation (2)).

$$\boldsymbol{\lambda}_t = \boldsymbol{\lambda}_{t-1} - \alpha \nabla L\left(\boldsymbol{\lambda}_{t-1}\right) + \tau\left(\boldsymbol{\lambda}_{t-1} - \boldsymbol{\lambda}_{t-2}\right) \tag{2}$$

Unlike SGDM that uses a fixed learning rate, RMSProp changes the learning rate over time with an exponentially decaying average that engages the squared gradients from the recent time steps (Equations (3)–(5)). The parameter γ controls the decay rates of the moving averages. The last changes to the network parameters in $\boldsymbol{\lambda}$ are represented by $\boldsymbol{\upsilon}_{t-1}$.

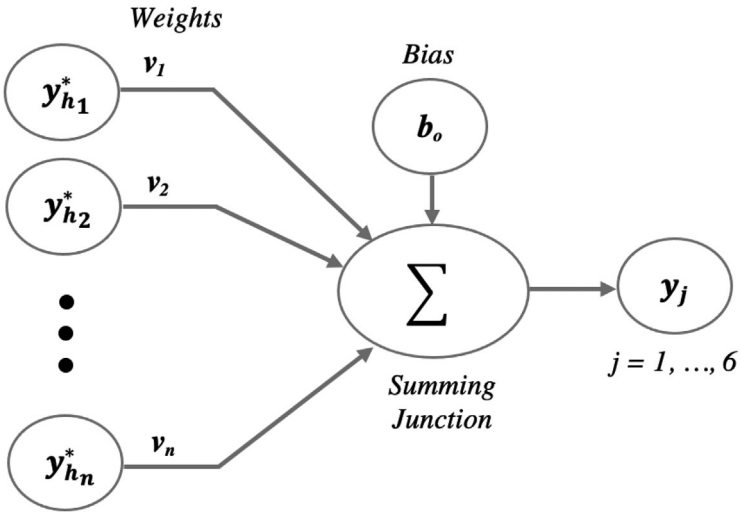

FIGURE 4 Transaction from the hidden layer to the output layer

$$\lambda_t = \lambda_{t-1} - \frac{\alpha \nabla L(\lambda_{t-1})}{\sqrt{\hat{v}_{t-1}} + \epsilon} \tag{3}$$

$$\hat{v}_{t-1} = \frac{v_{t-1}}{1 - \gamma_1^{t-1}} \tag{4}$$

$$v_{t-1} = (1 - \gamma_1)(\nabla L(\lambda_{t-1}))^2 + \gamma_1 v_{t-2} \tag{5}$$

Similarly, Adam adapts the learning rates based on the average of both the gradient magnitudes and the squared gradients from the recent time steps (Equations (6)–(8)).

$$\lambda_t = \lambda_{t-1} - \frac{\alpha . \hat{m}_{t-1}}{\sqrt{\hat{v}_{t-1}} + \epsilon} \tag{6}$$

$$\hat{m}_{t-1} = \frac{m_{t-1}}{1 - \gamma_2^{t-1}} \tag{7}$$

$$m_{t-1} = (1 - \gamma_2) \nabla L(\lambda_{t-1}) + \gamma_2 m_{t-2} \tag{8}$$

3.3 | Selection of training and testing data

Similar to other ML algorithms, the model performance is examined using a test data set that has not been used in training the model. To properly evaluate the performance of the model, the data are split into two sets of training (80%) and testing (20%). As shown in Figure 5, prediction accuracy improves as the training size of the data set increases up to a specific point. More particularly, increasing the training size from 70% to 95% of the entire data increases the accuracy of training prediction from 85.87% to 87.02%. Using more data points as the training set increases the prediction accuracy of the model up to a specific point after which the performance remains almost constant for the training set and decreases for the testing set. Therefore, the 80% allocation to the training set is found appropriate in order to make a balance between the training and testing accuracy.

During the training–validation process, the most suitable network architecture is identified by tuning parameters of the neural network and performing sensitivity analyses. The hyperparameters are set while training the models, using a grid-search method, by minimizing MSEs. More specifically, a grid of hyperparameters is used for each model, and the model is trained on the training set and validated using the validation set. In this process, the models are evaluated through a 10-fold cross-validation technique,[41] which is a common practice in ML to avoid overfitting. As schematically shown in Figure 6, this technique randomly partitions data into similar sized 10 subsets with an equal number of data points in

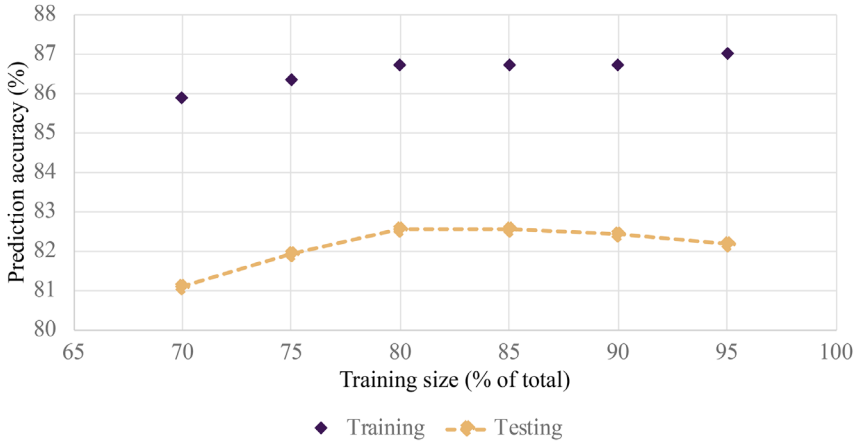

FIGURE 5 Variations of different training sizes in predicting y_1 (column curvature ductility) using stochastic gradient descent with momentum (SGDM)

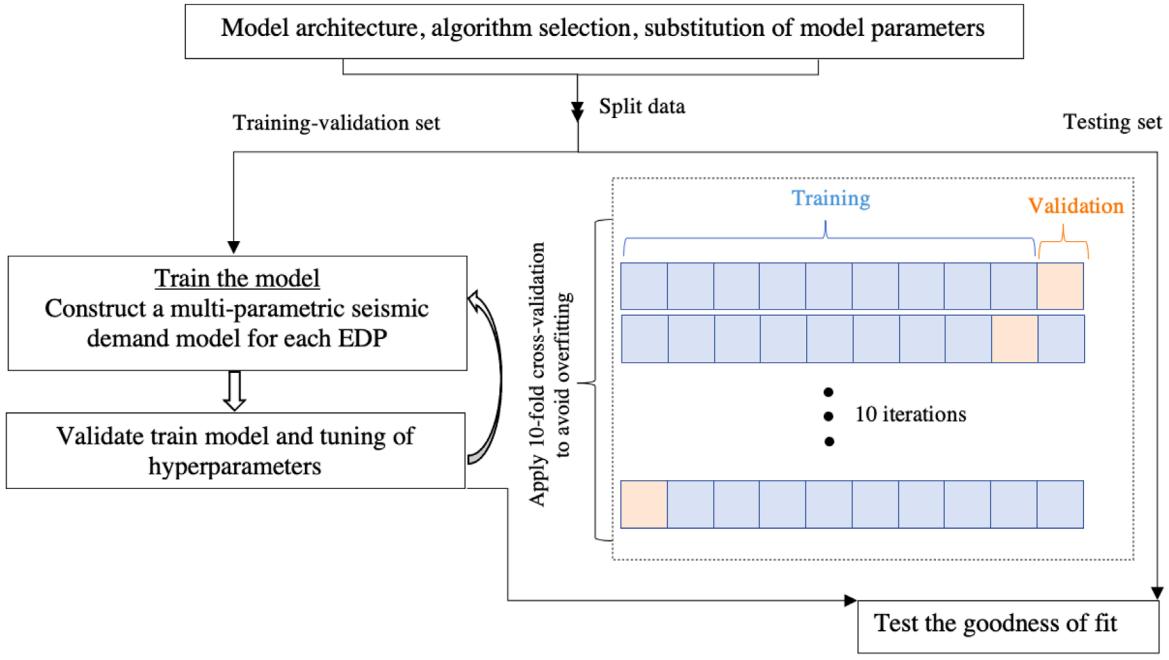

FIGURE 6 Process to train, validate, and test the artificial neural network (ANN)-based probabilistic seismic demand models (PSDMs)

each subset. Through an iterative process, the model is trained using nine subsets and is validated on the remaining 10th subset. This training–validation process is iterated 10 times. The prediction accuracy and the error term are computed in each iteration, and the average values across all folds are reported as the final values. The performance of the final generated model is evaluated and compared to the classical PSDM using the test set. Once the model is trained and tuned, the remaining 20% of the data (known as the testing set) is used to evaluate the performance of the final tuned models based on prediction accuracy and MSE.

4 | IMPLEMENTATION OF ANN

4.1 | Neural network architecture for bridge seismic demands

Using the aforementioned solvers in MATLAB, different types of neural networks are created for each seismic demand (y_i). Regarding the execution environment, this study uses GPU-based accelerated processing. In terms of the training options, the following features and hyperparameters are found the most suitable for the predictive models: 150 maximum number of epochs; mini-batch size 50; gradient decay factor 0.9; squared gradient decay factor, 0.9; L2 regularization 0.001;

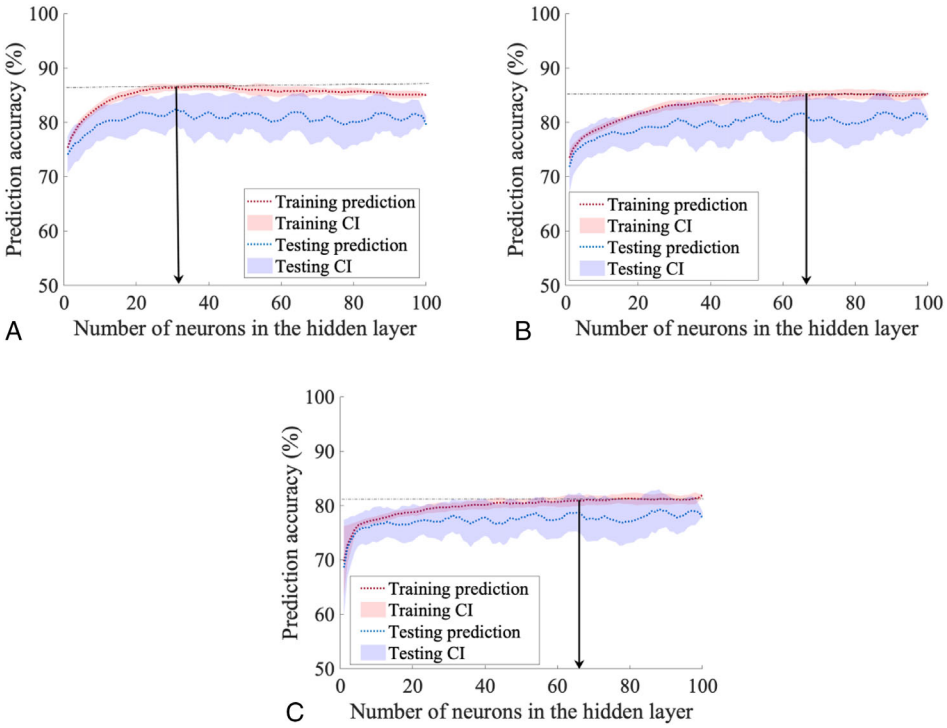

FIGURE 7 Comparison of the model performance based on prediction accuracy to predict y_1 (column curvature ductility) using: (A) stochastic gradient descent with momentum (SGDM), (B) root mean squared propagation (RMSProp), and (C) Adam

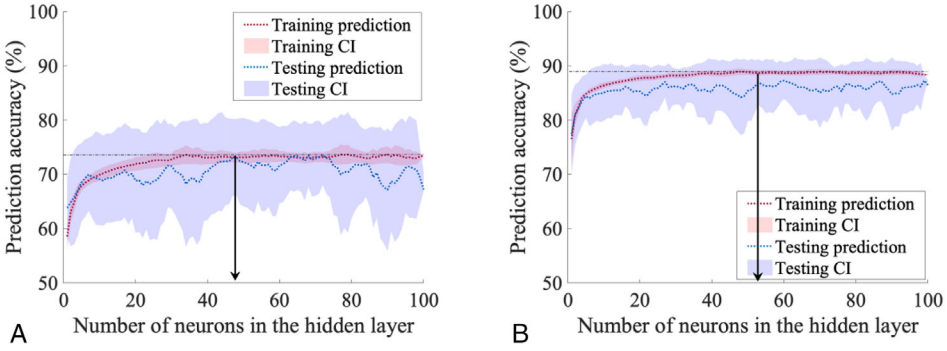

FIGURE 8 The most-viable predictive models for (A) y_2 (deck displacement) and (B) y_3 (foundation translational displacement) using the root mean squared propagation (RMSProp) solver

momentum 0.9; epsilon, 1e − 8. The initial learning rate that is used for the SGDM, RMSProp, and Adam is 0.01, 0.001, and 0.001, respectively.

For each network type, networks are constructed using a range of neurons varying from a single neuron to 100 neurons. In order to identify the most-viable number of neurons in the hidden layer, the prediction accuracy and MSE of the ANN models are evaluated for the training and testing datasets. Figures 7–10 display the performance variation of the ANN models, in terms of prediction accuracy and MSE along with their associated confidence intervals (CI), based on incorporating a different number of neurons. The most-viable numbers of neurons of different models are the numbers that resulted in the highest prediction accuracy or lowest MSE error (considering the overfitting issue and a proper balance between the training and testing prediction accuracy), indicated by vertical arrow lines in Figures 7–10 and summarized in Table 3. Compared to using a fixed set of 10 neurons in the hidden layer (as was the case with the previous studies), Figure 11 indicates that prediction accuracy improves when the most-viable neurons are identified and used in developing the ANN-based predictive models.

It is also observed that the model performance improves to a specific point after which increasing the number of neurons does not significantly influence the prediction, but with an expense of increasing model complexity, computational cost,

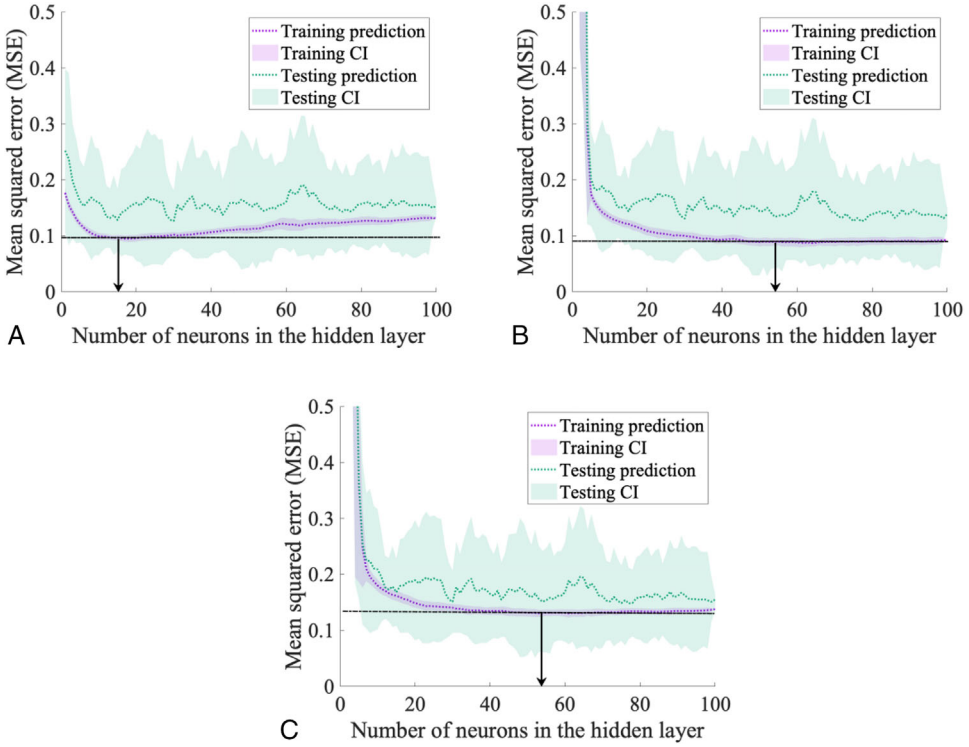

FIGURE 9 Comparison of the model performance based on mean squared error (MSE) to predict y_4 (foundation rotation) using: (A) stochastic gradient descent with momentum (SGDM), (B) root mean squared propagation (RMSProp), and (C) Adam

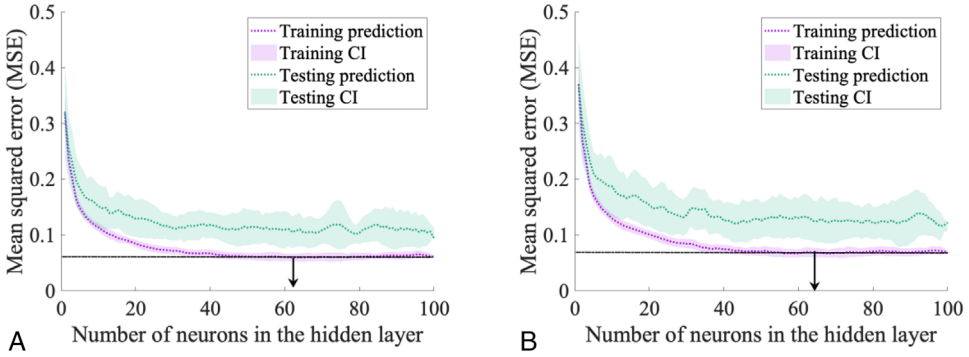

FIGURE 10 The most-viable predictive models for (A) y_5 (active abutment displacement) and (B) y_6 (passive abutment displacement) using the root mean squared propagation (RMSProp) solver

TABLE 3 Summary of the prediction accuracy values for the most-viable neural network architecture

		Most-viable number of neurons			Prediction accuracy (%)					
					Training			Testing		
	Solver	SGDM	RMSProp	Adam	SGDM	RMSProp	Adam	SGDM	RMSProp	Adam
Seismic demand	y_1	31	66	66	**86.71**	85.12	81.07	**82.69**	81.09	78.13
	y_2	30	48	42	71.34	**73.11**	72.52	70.30	**72.09**	71.55
	y_3	27	53	42	86.90	**88.49**	86.54	85.18	**86.52**	84.88
	y_4	15	54	54	95.72	**95.86**	94.98	94.74	**94.86**	94.49
	y_5	27	62	67	73.81	**80.70**	77.07	66.95	**75.43**	73.46
	y_6	25	64	67	74.68	**81.22**	77.55	72.32	**75.90**	71.53

Abbreviations: RMSProp, root mean squared propagation; SGDM, stochastic gradient descent with momentum.

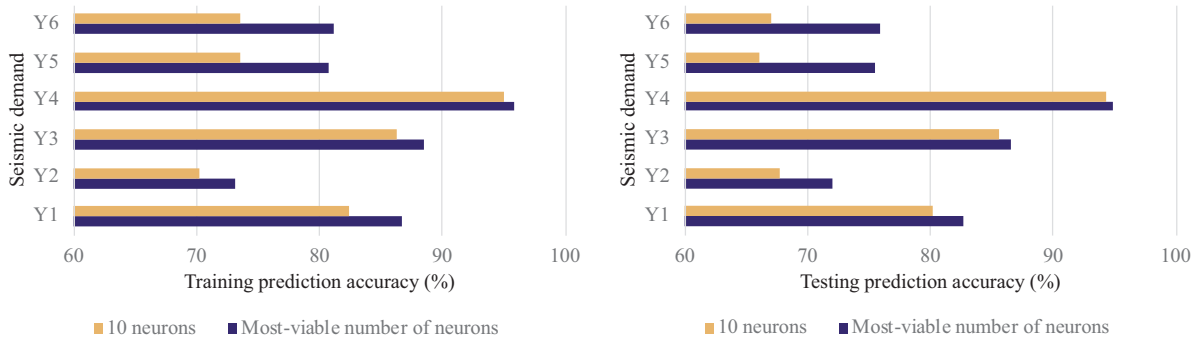

FIGURE 11 Comparison of the performance of models with 10 neurons and the most-viable number of neurons found in this study (Table 3)

FIGURE 12 Illustration of classical

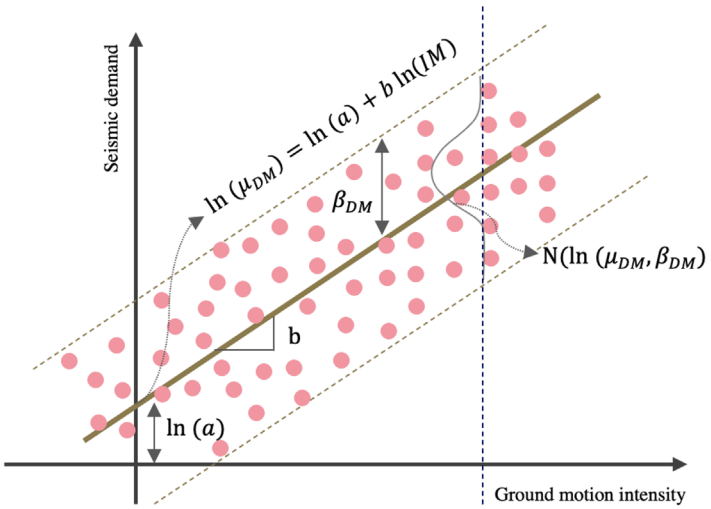

and the possibility of overfitting. As an example, to predict the column curvature ductility using the ANN model that is developed based on SGDM, the accuracy increases from ~74% by adopting a single neuron to ~86% using 30 neurons (Figure 7(A)). As indicated by an arrow in the plot, 31 is identified as the most-viable number of neurons in the hidden layer for the predictive ANN model that was developed using SGDM. For the investigated seismic demands, Table 3 presents a summary of the results for the prediction accuracies corresponding to the most-viable number of neurons for each solver. Bolded numbers indicate the highest accuracy for each output variable during training and testing. Furthermore, initial analyses indicated that using two and three hidden layers does not noticeably change the results, and thus a single hidden layer was adopted for the remaining analyses.

4.2 | Final proposed models

Based on the presented results, in the previous section, from the sensitivity study, the hyperparameters selected for the ANN models are: the SGDM solver and 31 neurons for estimating the column curvature ductility (y_1), and the RMSProp solver and 48 neurons for estimating the deck displacement (y_2). For the other demands corresponding to the foundation and abutment, RMSProp is found as the best solver and the most-viable number of neurons are 53, 54, 62, and 64 for y_3 to y_6, respectively.

Moreover, the normalization of the input variables improved the overall performance of the models, so the Z-score normalization was adapted to the models. In terms of the activation functions,[42] sigmoid (Equation (9)), which is considered for developing the final models, performed slightly better than the rectified linear unit (ReLU) for the studied neural

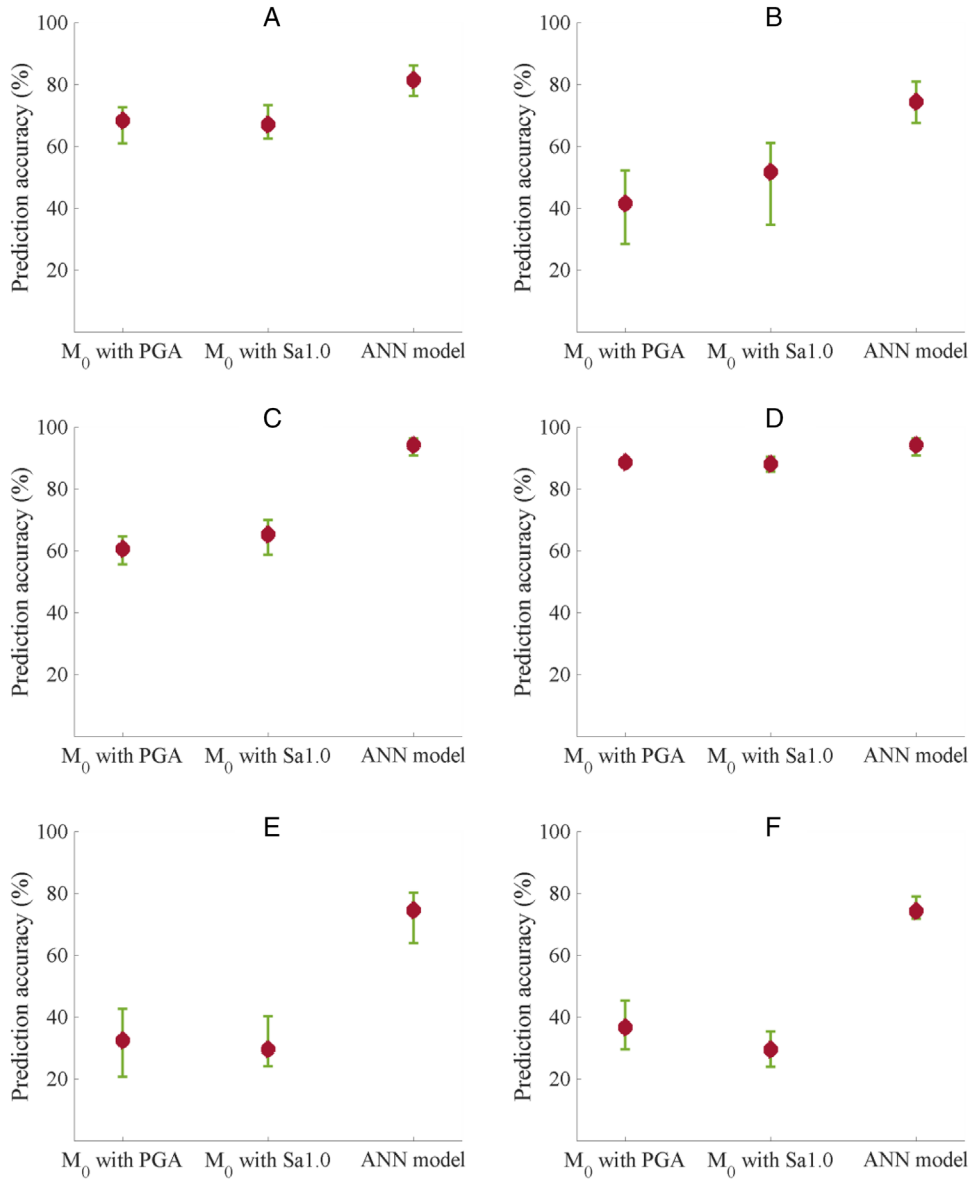

FIGURE 13 Comparison of the prediction accuracy of the artificial neural network (ANN)-based models with the classical probabilistic seismic demand models (PSDMs) for: (A) y_1 (column curvature ductility), (B) y_2 (deck displacement), (C) y_3 (foundation translational displacement), (D) y_4 (foundation rotation), (E) y_5 (active abutment displacement), (F) y_6 (passive abutment displacement)

network architecture.

$$f\left(y_{h_i}\right) = 1/\left(1 + \exp\left(-y_{h_i}\right)\right) \tag{9}$$

The hidden layer is comprised of neurons that link the input to the output dataset. The ANN-based predictive model is formulated according to the transaction from the variables in the input layer to the neurons in the hidden layer (Figure 3) and the transformation of the outputs of the hidden layer to the output layer (Figure 4). The final model is expressed as in Equation (10), while the corresponding values of weights and biases, developed through training, are reported in Appendix – B (Table B.1) for selective responses.

$$y_j = (b_o)_j + \sum_{i=1}^{n} (v_i)_j [1/1 + \exp(-[(w_{1,i})_j x_1 + (w_{2,i})_j x_2 + \cdots + (w_{34,i})_j x_{34} + (b_i)_j])] \tag{10}$$

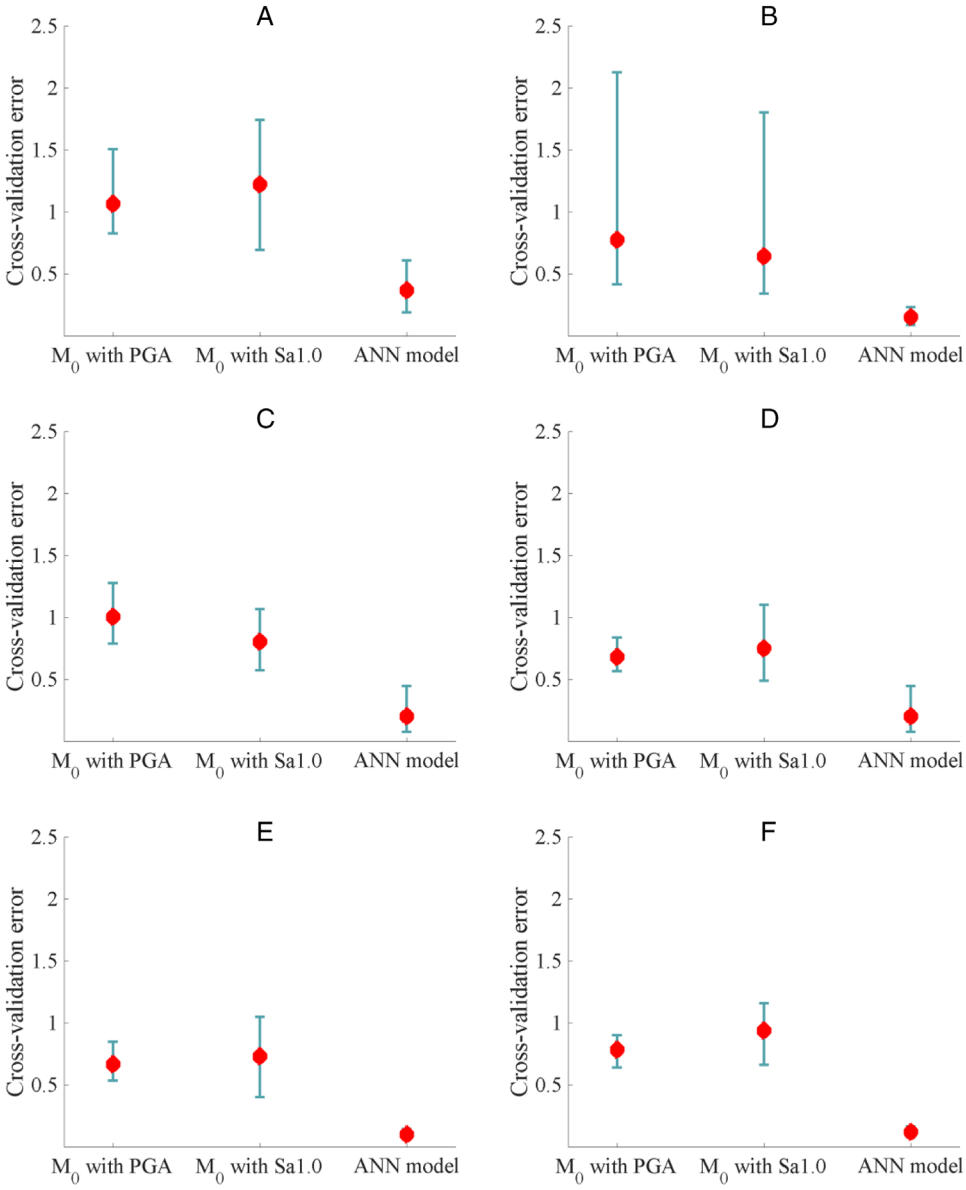

FIGURE 14 Comparison of the cross-validation errors of the artificial neural network (ANN)-based models with the classical probabilistic seismic demand models (PSDMs) for: (A) y_1 (column curvature ductility), (B) y_2 (deck displacement), (C) y_3 (foundation translational displacement), (D) y_4 (foundation rotation), (E) y_5 (active abutment displacement), (F) y_6 (passive abutment displacement)

5 | COMPARISON OF ANN MODEL AND CLASSICAL REGRESSION MODEL

The median estimate of the structural demand ($\tilde{S}_D$) based on the classical approach was formed by a power-law model as

$$\boldsymbol{\mu}_{\tilde{S}_D} = a(\boldsymbol{IM})^b \tag{11}$$

where a and b are the regression coefficients.[1,43] IM represents the intensity measure of the ground motions. PGA and spectral acceleration at 1.0 s (Sa(1.0s)) are typically used as the IMs for bridge applications.[12,44–46] The classical PSDM introduced in Equation (11) is equivalent to a linear regression fit model (Figure 12) in the natural logarithmic coordinate space, and therefore can be represented as Equations (12) and (13).

$$\ln(\boldsymbol{\mu}_{DM}) = \ln(a) + b\ln(\boldsymbol{IM}) \tag{12}$$

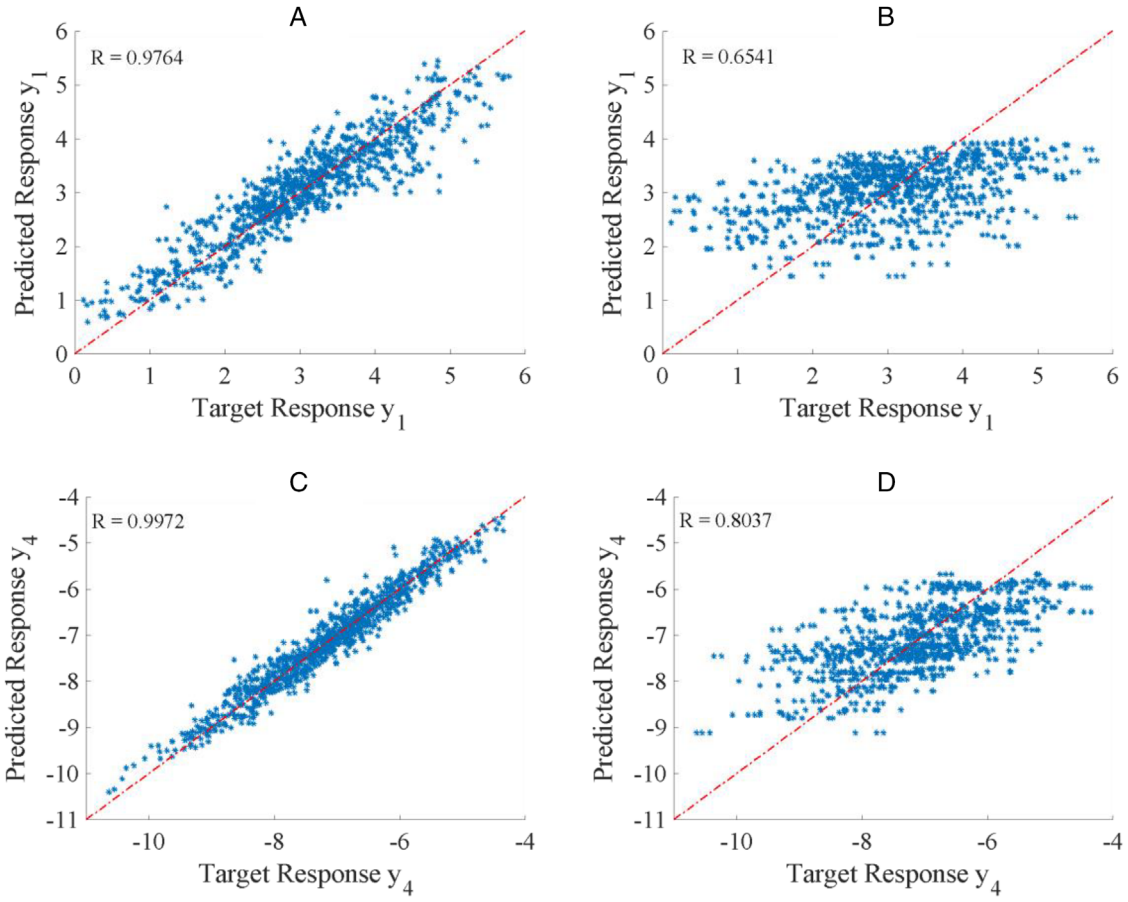

FIGURE 15 Comparison of seismic demands predicted by regression models and computed by finite element analysis for: (A) y_1 predicted by artificial neural network (ANN)-based model, (B) y_1 predicted by classical model, (C) y_4 predicted by ANN-based model, and (D) y_4 predicted by classical model

$$\beta_{DM} = \sqrt{\frac{\sum_{i=1}^{m}\left[\ln\left(S_{D_i}\right) - \left(\ln\left(a\right) + bln\left(IM_i\right)\right)\right]^2}{m-2}} \tag{13}$$

In these formulations, S_D represents the value of seismic demand obtained from the nonlinear dynamic analysis performed in OpenSees, and m shows the total number of recorded responses.

For the performance assessment of the ANN approach, the predictions from the proposed ANN-based model are compared with those from the classical model (M_0) which is developed using the traditional regression techniques. As presented in Figures 13 and 14, the ANN-based models provide a better approximation of the demands by improving the prediction accuracy and reducing cross-validation errors. The largest improvement (around 85% reduction in the cross-validation error) is observed for predicting the displacement of the abutments (Figures 13(E) and 13(F)). Besides, moderate improvements are noted for the other responses (65%–75% error reduction). The lowest increase in the prediction accuracy is found for the foundation rotation where both approaches well approximated the median demand with ~88% and ~94% accuracy computed using the classical model and the ANN model, respectively.

Figure 15 displays the correlation between the predicted median seismic demands and the targeted responses simulated using the finite element dynamic analysis. In the case of the ANN-based models, shown in Figures 15(A) and 15(C), the predictions and target responses are mostly centered around the 1:1 line resulting in high values of R (e.g., R~0.97 for y_1). As this plot compares the predictions from the ANN-based models (Figures 15(A) and 15(C)) and the classical models (Figures 15(B) and 15(D)), the largest differences appear over the medium range of small and large responses where the ANN-based models can efficiently capture the nonlinearity in the data while the classical model with the linearity assumption can not capture this complexity. The high R values (Figure 15) and low cross-validation errors (Figure 14) indicate that the proposed ANN-based models are generalizable.

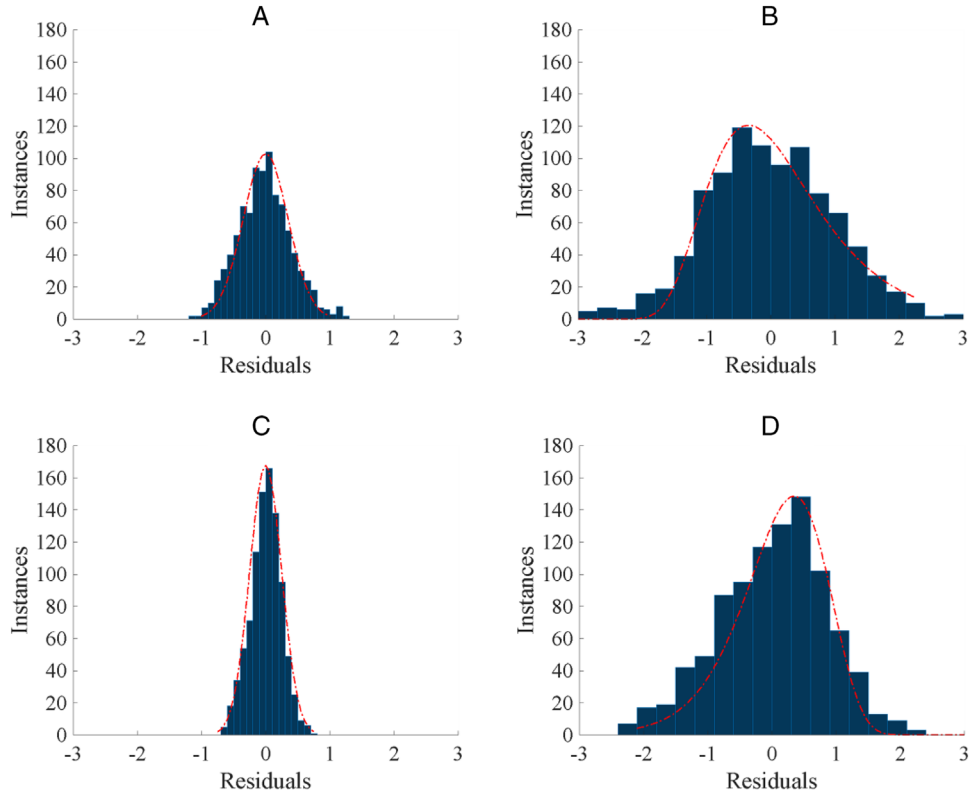

FIGURE 16 Distribution of residuals for the predicted responses of (A) y_1 from artificial neural network (ANN)-based model, (B) y_1 from classical model, (C) y_4 from ANN-based model, and (D) y_4 from classical model

TABLE 4 The list of compared models including the classical and common algorithms

Models	Algorithms	Terms	Formulation
M0 with PGA	Classic regression model	1st order	$y_i = \alpha_{0_i} + b_i \ln(PGA)$
M0 with Sa1.0	Classic regression model	1st order	$y_i = \alpha_{0_i} + b_i \ln(Sa1.0)$
M1	Multiparameter regression model	1st order	$y_i = \alpha_{0_i} + \sum_{j=1}^{m} \alpha_{j_i} x_j$
M2	2nd-order polynomial	2nd order	$y_i = \alpha_{0_i} + \sum_{j=1}^{m} \alpha_{j_i} x_j^2$
M2-S	2nd-order polynomial	2nd order	$y_i = \alpha_{0_i} + \sum_{j=1}^{m} \alpha_{j_i} x_j^2$ (with stepwise regression)
M3	2nd-order polynomial	1st and 2nd order and interactive	$y_i = \alpha_{0_i} + \sum_{j=1}^{m} \alpha_{j_i} x_j + \sum_{j=1}^{m} \alpha_{jj_i} x_j^2 + \sum_{j=1}^{m} \sum_{l=2,l>j}^{m} \alpha_{jl_i} x_j x_l$
M4	2nd-order polynomial	1st and 2nd order	$y_i = \alpha_{0_i} + \sum_{j=1}^{m} \alpha_{j_i} x_j + \sum_{j=1}^{m} \alpha_{jj_i} x_j^2$
M4-S	2nd-order polynomial	1st and 2nd order	$y_i = \alpha_{0_i} + \sum_{j=1}^{m} \alpha_{j_i} x_j + \sum_{j=1}^{m} \alpha_{jj_i} x_j^2$ (with stepwise regression)

Besides, residuals are compared in Figure 16 to check the variability in the demand predictions. In the case of ANN model predictions (Figures 16(A) and 16(C)), as the fitted distributions (dashed red lines) indicate, the residuals are normally distributed with a mean close to zero. However, the residuals obtained from the predictions of the classical models (Figures 16(B) and 16(D)) do not satisfy these criteria indicating a noticeable bias associated with this type of model. The mean residuals of the classical models are 0.82 and 0.78 for the examples shown in Figures 16(B) and 16(D), and the highest frequency of residuals belongs to the [−0.6, −0.3] and [0.3, 0.6] bins, respectively. Overall, the results imply the unbiased predictions of the ANN-based models compared to the classical models since the residuals of the ANN models are closer to zero but there is a noticeable randomly distributed residual associated with the classical models.

Moreover, the performance of the ANN-based model is compared with the other common alternative forms of PSDMs such as the classical regression models (single parameter models with either PGA or Sa1.0), multiparameter linear regression model (using the input variables in Table 1), and the variations of 2nd-order polynomial regression models (see Table 4). Figure 17 displays a comparison of the accuracy of predictions obtained from these models. In general, it is

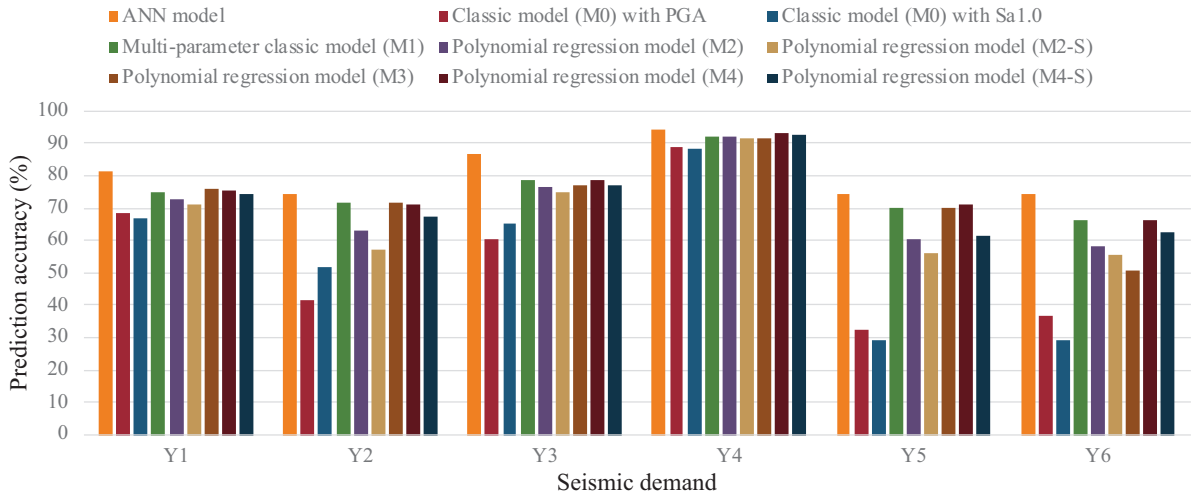

FIGURE 17 Comparison of the performance of the artificial neural network (ANN)-based model and the common regression-based probabilistic seismic demand models (PSDMs)

noted that including multiple uncertain parameters, in the form of multiparameter and 2nd-order polynomial regression model, leads to better estimation of the demands. The performance of the polynomial models depends on the seismic demand of interest. In particular, the 2nd-order polynomial models, which include both 1st- and 2nd-order terms with or without the interactive terms performed better than the other polynomial forms. Overall, it is observed that, in predicting all seismic demands, the ANN-based model outperforms the other regression-based models (Figure 17).

6 | CONCLUSIONS

The functional form of PSDMs becomes complex by adding uncertainty treatment as the number of input variables increases. ML algorithms that are capable of capturing complex interactions between the random variables involved in the bridge seismic analysis and the estimated seismic demands provide appealing alternatives to the classical demand models. Despite the emerging advancements in ML approaches, many of them have not yet been introduced to estimate bridge seismic responses.

This study implements a gradient descent ANN to develop predictive models for the probabilistic seismic demands corresponding to the key bridge components. The established network incorporated 34 input variables to cover the associated uncertainties in the ground motion and structural modeling parameters to predict six seismic demands corresponding to the column, deck, foundation, and abutment. Three different solvers including Adam, RMSProp, and SGDM were explored, and sensitivity analysis was conducted to identify the most appropriate hyperparameters of the network's architecture.

It is found that the proposed ANN algorithm efficiently modeled complex interaction and nonlinear characteristics inherent in the probabilistic seismic demands, and no systematic bias was observed in the developed ANN-based models. Moreover, compared with the classical regression-based model, the ANN-based model better captured the small and large values of the median seismic demands. The role of ANN in providing an alternative PSDM is imperative to provide a more reliable estimation of the bridge vulnerability when subjected to an earthquake. Particularly, the ANN-based PSDMs can be incorporated with the capacity limits to generate fragility curves for the bridge components.

Forthcoming studies, focusing on the vulnerability assessment of the bridge system, need to account for the correlation between the component vulnerabilities to integrate the component fragilities in order to develop the system-level bridge fragility curves. Although the findings from this study pave the path towards the application of ANN-based approaches to have a more reliable prediction of the demands, the limitations of this study can be addressed in future works. The results of this study may be limited to cohorts of bridges considered; however, future work will investigate the repeatability of the findings on other bridge classes such as I-girder, T-girder, and Slab bridges. Besides, future studies may explore to what extend the bridge system fragilities are sensitive to the different characteristics of the ANN-based PSDMs.

DATA AVAILABILITY STATEMENT

The data that support the findings of this study are available from the corresponding author upon reasonable request.

ORCID

Farahnaz Soleimani https://orcid.org/0000-0001-7809-2978

REFERENCES

1. Cornell CA, Jalayer F, Hamburger RO, Foutch DA. Probabilistic basis for 2000 SAC Federal Emergency Management Agency steel moment frame guidelines. *J Struct Eng*. 2002;128(4):526–533.
2. Seo J, Linzell DG. Use of response surface metamodels to generate system level fragilities for existing curved steel bridges. *Eng Struct*. 2013;52:642–653.
3. Ghosh J, Padgett JE, Dueñas-Osorio L. Surrogate modeling and failure surface visualization for efficient seismic vulnerability assessment of highway bridges. *Probab Eng Mech*. 2013;34:189–199.
4. Soleimani F, Vidakovic B, DesRoches R, Padgett J. Identification of the significant uncertain parameters in the seismic response of irregular bridges. *Eng Struct*. 2017;141:356–372.
5. Xie Y, Zhang J, DesRoches R, Padgett JE. Seismic fragilities of single-column highway bridges with rocking column-footing. *Earthquake Engineering & Structural Dynamics*. 2019;48(7):843–864.
6. Soleimani F. Propagation and quantification of uncertainty in the vulnerability estimation of tall concrete bridges. *Eng Struct*. 2020;202:109812.
7. Xie Y, DesRoches R. Sensitivity of seismic demands and fragility estimates of a typical California highway bridge to uncertainties in its soil-structure interaction modeling. *Eng Struct*. 2019;189:605–617.
8. Soleimani F. Analytical seismic performance and sensitivity evaluation of bridges based on random decision forest framework. *Structures*. 2021;32:329–341.
9. Mangalathu S, Heo G, Jeon JS. Artificial neural network based multi-dimensional fragility development of skewed concrete bridge classes. *Eng Struct*. 2018;162:166–176.
10. Pan Y, Agrawal AK, Ghosn M. Seismic fragility of continuous steel highway bridges in New York State. *J Bridge Eng*. 2007;12(6):689–699.
11. Seo J, Park H. Probabilistic seismic restoration cost estimation for transportation infrastructure portfolios with an emphasis on curved steel I-girder bridges. *Struct Saf*. 2017;65:27–34.
12. Freddi F, Padgett JE, Dall'Asta A. Probabilistic seismic demand modeling of local level response parameters of an RC frame. *Bull Earthq Eng*. 2017;15(1):1–23.
13. Mangalathu S, Jeon JS. Stripe-based fragility analysis of multispan concrete bridge classes using machine learning techniques. *Earthq Eng Struct Dyn*. 2019;48(11):1238–1255.
14. Xie Y, Ebad Sichani M, Padgett JE, DesRoches R. The promise of implementing machine learning in earthquake engineering: a state-of-the-art review. *Earthq Spectra*. 2020;36(4):1769–1801.
15. Shokri M, Tavakoli K. A review on the artificial neural network approach to analysis and prediction of seismic damage in infrastructure. *Int J Hydromechatronics*. 2019;2(4):178–196.
16. Lagaros ND, Fragiadakis M. Fragility assessment of steel frames using neural networks. *Earthq Spectra*. 2007;23(4):735–752.
17. Mitropoulou CC, Papadrakakis M. Developing fragility curves based on neural network IDA predictions. *Eng Struct*. 2011;33(12):3409–3421.
18. Ferrario E, Pedroni N, Zio E, Lopez-Caballero F. Bootstrapped artificial neural networks for the seismic analysis of structural systems. *Struct Saf*. 2017;67:70–84.
19. Wang Z, Pedroni N, Zentner I, Zio E. Seismic fragility analysis with artificial neural networks: application to nuclear power plant equipment. *Eng Struct*. 2018;162:213–225.
20. Khosravikia F, Kurkowski J, Clayton P. Fragility of masonry veneers to human-induced Central U.S. earthquakes using neural network models. *J Build Eng*. 2020;28:101100.
21. Kim T, Song J, Kwon O-S. Probabilistic evaluation of seismic responses using deep learning method. *Struct Saf*. 2020;84:101913.
22. Pang Y, Dang X, Yuan W. An artificial neural network based method for seismic fragility analysis of highway bridges. *Adv Struct Eng*. 2014;17(3):413–428.
23. Rafiq MY, Bugmann G, Easterbrook DJ. Neural network design for engineering applications. *Comput Struct*. 2001;79(17):1541–1552.
24. Soleimani F, Mangalathu S, DesRoches R. A comparative analytical study on the fragility assessment of box-girder bridges with various column shapes. *Eng Struct*. 2017;153:460–478.
25. McKenna F. OpenSees: a framework for earthquake engineering simulation. *Comput Sci Eng*. 2011;13(4):58–66.
26. Soleimani F. Pattern recognition of the seismic demands for tall pier bridge systems. *J Earthq Eng*. 2021:1–19. https://doi.org/10.1080/13632469.2021.1927894
27. Soleimani F. Fragility of California Bridges-Development of Modification Factors [doctoral dissertation]. Georgia Institute of Technology. 2017.
28. Baker JW, Lin T, Shahi SK, Jayaram N. *New Ground Motion Selection Procedures and Selected Motions for the PEER Transportation Research Program*. Pacific Earthquake Engineering Research Center; 2011.

29. Hill T, Marquez L, O'Connor M, Remus W. Artificial neural network models for forecasting and decision making. *Int J Forecast*. 1994;10(1):5–15.
30. Kartam N, Flood I, Garrett JH. *Artificial Neural Networks for Civil Engineers: Fundamentals and Applications*. New York, NY: American Society of Civil Engineers; 1997.
31. Sarle WS. Neural networks and statistical models. 1994.
32. Amari SI. Backpropagation and stochastic gradient descent method. *Neurocomputing*. 1993;5(4–5):185–196.
33. Bottou L. Stochastic gradient learning in neural networks. In: *Proceedings of Neuro-Nımes*. 1991;91(8):12.
34. Bottou L. Stochastic gradient descent tricks. In: *Neural Networks: Tricks of the Trade*. Berlin, Heidelberg: Springer; 2012:421–436.
35. Cao, Y., & Gu, Q. Generalization bounds of stochastic gradient descent for wide and deep neural networks. Advances in Neural Information Processing Systems, 2019; 32, 10836-10846.
36. Cilimkovic M. *Neural Networks and Back Propagation Algorithm*. Vol. 15. North Dublin: Institute of Technology Blanchardstown; 2015:1–12.
37. Benardos PG, Vosniakos GC. Optimizing feedforward artificial neural network architecture. *Eng Appl Artif Intell*. 2007;20(3):365–382.
38. Kingma, D. P., Ba, J. Adam: A method for stochastic optimization. 2014; arXiv preprint arXiv:1412.6980.
39. Gitman, I., Lang, H., Zhang, P., Xiao, L. Understanding the role of momentum in stochastic gradient methods. 2019; arXiv preprint arXiv:1910.13962.
40. Takase T, Oyama S, Kurihara M. Effective neural network training with adaptive learning rate based on training loss. *Neural Netw*. 2018;101:68–78.
41. Hastie T, Tibshirani R, Friedman J. *The Elements of Statistical Learning: Data Mining, Inference, and Prediction*. New York, NY: Springer Science & Business Media; 2009.
42. Sharma S. *Activation Functions in Neural Networks*. Towards Data Science. 2017:6.
43. Shome N, Cornell CA, Bazzurro P, Carballo JE. Earthquakes, records, and nonlinear responses. *Earthq Spectra*. 1998;14(3):469–500.
44. Ma HB, Zhuo WD, Lavorato D, et al. Probabilistic seismic response and uncertainty analysis of continuous bridges under near-fault ground motions. *Front Struct Civ Eng*. 2019;13(6):1510–1519.
45. Padgett JE, Nielson BG, DesRoches R. Selection of optimal intensity measures in probabilistic seismic demand models of highway bridge portfolios. *Earthq Eng Struct Dyn*. 2008;37(5):711–725.
46. Ramanathan K. Next Generation Seismic Fragility Curves for California Bridges Incorporating the Evolution in Seismic Design Philosophy *[doctoral dissertation]*. Georgia Institute of Technology; 2012.
47. Cornell CA, Krawinkler H. Progress and challenges in seismic performance assessment. *PEER Ctr News*. 2000;3(2):1–2.

SUPPORTING INFORMATION

Additional supporting information may be found in the online version of the article at the publisher's website.

How to cite this article: Soleimani F, Liu X. Artificial neural network application in predicting probabilistic seismic demands of bridge components. *Earthquake Engng Struct Dyn*. 2021;1–18. https://doi.org/10.1002/eqe.3582